Synthesis of Polyethylene-Octene Elastomer/SiO_2-TiO_2 Nanocomposites via In Situ Polymerization: Properties and Characterization of the Hybrid

CHIN-SAN WU

Department of Biochemical & Institute of Environmental Polymer Materials, Kao Yuan Institute of Technology, Kaohsiung County, Taiwan 82101, Republic of China

Received 8 July 2004; accepted 9 November 2004
DOI: 10.1002/pola.20649
Published online in Wiley InterScience (www.interscience.wiley.com).

ABSTRACT: In this study, a silicic acid and tetra isopropyl ortho titanate ceramic precursor and a metallocene polyethylene-octene elastomer (POE) or acrylic acid grafted metallocene polyethylene-octene elastomer (POE-g-AA) were used in the preparation of hybrids (POE/SiO_2-TiO_2 and POE-g-AA/SiO_2-TiO_2) using an *in situ* sol-gel process, with a view to identifying a hybrid with improved thermal and mechanical properties. Hybrids were characterized using Fourier transform infrared spectroscopy, ^{29}Si solid-state nuclear magnetic resonance (NMR), X-ray diffraction, differential scanning calorimetry, thermogravimetry analysis, dynamic mechanical thermal analysis, and Instron mechanical testing. Properties of the POE-g-AA/SiO_2-TiO_2 hybrid were superior to those of the POE/SiO_2-TiO_2 hybrid. This was because the carboxylic acid groups of acrylic acid acted as coordination sites for the silica-titania phase to allow the formation of stronger chemical bonds. ^{29}Si solid-state NMR showed that Si atoms coordinated around SiO_4 units were predominantly Q_3 and Q_4. The 10 wt % SiO_2-TiO_2 hybrids gave the maximum values of tensile strength and glass transition temperature in both POE/SiO_2-TiO_2 and POE-g-AA/SiO_2-TiO_2. It is proposed that above this wt %, excess SiO_2-TiO_2 particles caused separation between the organic and inorganic phases. © 2005 Wiley Periodicals, Inc. J Polym Sci Part A: Polym Chem 43: 1690–1701, 2005

Keywords: *in situ* polymerization, nanocomposites, POE-g-AA/SiO_2-TiO_2 hybrid, sol-gel

INTRODUCTION

The synergistic combination of polymers and ceramics via a sol-gel process has recently attracted great attention in the field of material science because, by manipulating structure at a molecular level, it has the potential for developing new materials with desired properties.[1–12] These new hybrid materials could have a controllable combination of the benefits of polymers (such as flexibility, toughness, and ease of processing) and those of ceramics or glasses (such as hardness, durability, and thermal stability). Research on organic–inorganic composites has primarily focused on inorganic modification of an organic polymer dominant phase.[13,14] Specifically, the polymeric phases commonly used in sol-gel processed ceramic-reinforced polymers are elastomers, glassy polymers, semicrystalline polymers, and other polymeric media, such as membranes of perfluorosulfonic acid (Naflon®).[15] Organometallic compounds ($M[OC_nH_{2n+1}]_2$, M = Si, Ti, Sn, Al, etc.) are generally used as the ceramic pre-

Correspondence to: C.-S. Wu (E-mail: cws1222@cc.kyit.edu.tw)
Journal of Polymer Science: Part A: Polymer Chemistry, Vol. 43, 1690–1701 (2005)

cursor, tetraethoxysilane (TEOS) being the most commonly used.[7,16,17]

The microstructures and the properties of hybrid materials depend greatly on the particle size of the inorganic phase, the uniform distribution of the inorganic phase within the organic phase, and the interfacial force between the two phases. The formation of hydrogen or covalent bonds between the two phases is normally utilized to establish this interfacial force.[18,19] Hydrogen bonds may arise from the basic group of the hydrogen acceptor in the polymer and the hydroxy group of the intermediate species from metal alkoxides. Alternatively, covalent bonds may form through dehydration of hydroxy groups in the polymer with residual Si–OH/Ti–OH groups in the SiO_2-TiO_2 network.

Polyethylene is one of the most important thermoplastics, but its use is restricted in certain applications by its low melting point, its stability, and a tendency to crack when stressed. To mitigate such disadvantages, the grafting reactions of polyethylene, its crosslinking reactions, and its blending with organic fillers have been extensively investigated for many years. Recently, the metallocene based polyethylene-octene elastomer (POE), which has been developed by Dow and Exxon using a metallocene catalyst, has received much attention due to its unique uniform distribution of comonomer and narrow molecular weight distribution.[20,21] Moreover, prompted by the observations of Kaempfer et al.[22] on the synthesis and characterization of maleated polypropylene/silicate nanocomposites, the performance of POE/silica was investigated by us in a previous work.[4]

With a view to further improving the thermal and mechanical properties of the ceramic polymer hybrid, in this study POE was blended with silica and titania through a sol-gel process. Formation and dispersion of the silica and titania network in the POE matrix was achieved using a new method, in which the formation of the inorganic phase was via an *in situ* polymerization of silicic acid and tetra isopropyl ortho titanate in the presence of polyethylene-octene elastomer. In addition, an acrylic acid grafted version of POE (POE-g-AA) was also investigated, on the presumption that carboxylic acid groups on this POE copolymer would react with residual silanol groups of the silica network and residual titanium bonded isopropyl groups of the titania network. The hybrid products (POE/SiO_2-TiO_2 and POE-g-AA/SiO_2-TiO_2) were characterized by Fourier transform infrared (FTIR) spectroscopy, ^{29}Si solid-state nuclear magnetic resonance (NMR) spectrometry, and X-ray diffraction (XRD). Moreover, the thermal and mechanical properties of the hybrids were examined using Dynamic Mechanical Analysis (DMA), thermogravimetry analysis (TGA), differential scanning calorimetry (DSC), and Instron mechanical testing.

EXPERIMENTAL

Materials

POE, with 18% octane (Engage 8003, Dow Chemical Co.) and sodium metasilicate hydrate, $Na_2SiO_3 \cdot 9H_2O$ (SMS, Merck Chemical Co.) were used as received. Acrylic acid (AA, Aldrich Chemical Co.) was purified before use by re-crystallization from chloroform. Tetra isopropyl ortho titanate (TTIP-$Ti[OCH(CH_3)_2]_4$, >97%) was obtained from the Merck Chemical Corp. The initiator dicumyl peroxide (DCP, Aldrich Chemical Co.) was recrystallized twice by dissolving it in absolute methanol, filtering the solution while hot, and chilling it in iced water. Other reagents were purified using the conventional methods. The POE-g-AA copolymer was made in our laboratory, and its grafting percentage was about 5.65 wt %.

Sample Preparation

POE-g-AA Copolymer

The grafting of AA onto molten POE was performed using xylene as an interface agent and DCP as an initiator under a nitrogen atmosphere at 85 ± 2 °C. A mixture of AA and DCP was added to the molten POE in four equal portions at 2-min intervals and with a rotor speed of 60 rpm. More detail regarding preparation and characterization of the POE-g-AA copolymer is given in our previous paper.[19] The grafting percentage was determined by a titration method[21] as being about 5.65 wt % with a DCP loading of 0.3 wt % and AA loading of 10 wt %.

POE/SiO_2-TiO_2 and POE-g-AA/SiO_2-TiO_2 Hybrids

The method proposed by Abe and Misono[23] was used to prepare the silicic acid-THF solution from sodium metasilicate hydrate. The sodium metasilicate hydrate aqueous solution (60 g of SMS in 150 mL of water) was added dropwise into 150 mL of hydrochloric acid (3.6mol/L) over a few minutes

Table 1. Compositions of Sol-Gel Liquid Solutions Used for the Preparation of Hybrid Materials

SiO_2-TiO_2 (wt %)	3	7	10	13	20
POE or POE-g-AA (g)	38.80	37.20	36.00	34.80	32.00
Sol A (ml)	7.68	17.92	25.60	33.28	51.20
TTIP (g)	2.63	4.97	7.09	9.22	14.19
Isopropanol/[TTIP][a]	17	17	17	17	17
Sol B					
[acetic acid]/[TTIP][a]	0.01	0.01	0.01	0.01	0.01
[HCl]/[TTIP][a]	0.08	0.08	0.08	0.08	0.08
[H_2O]/[TTIP][a]	4.0	4.0	4.0	4.0	4.0

[a] The weight ratio SiO_2/TiO_2 = 1:1.
[b] The mole ratio of isopropanol, acetic acid, HCl, and H_2O to TTIP.

with stirring at 0 °C, followed by further stirring for 15 min. Thereafter, 150 mL of THF and then 90 g of sodium chloride were added to this solution, again with stirring. After 30 min reaction, the solution, left to stand for 10 min, became two immiscible phases. The organic layer, silicic acid-THF solution designated as "Sol A," was separated out and dried with 30 g of anhydrous sodium sulfate. The silicic acid-THF solution extracted contained about 78.1 g/L of SiO_2.[24,25] Composition of sol-gel solutions, including volume of Sol A, used in preparing hybrids is shown in Table 1.

The mixture called "Sol B" was prepared by dissolving a stoichiometric amount of TPIP, H_2O, HCl (as the catalyst), and acetic acid in isopropanol (Table 1) and then stirring at room temperature for 30 min to obtain a homogeneous solution. The two solutions (A and B) were mixed at a SiO_2/TiO_2 weight ratio of 1:1. The final mixture was stirred for 25 h at room temperature. A set amount of POE or POE-g-AA (Table 1) was melted in a Brabender "Platograph" 200 Nm Mixer W50EHT instrument with a blade type rotor (50 rpm) and a temperature of 160–170 °C. When the POE or POE-g-AA had melted completely, the SiO_2/TiO_2 was added into the mixer to allow *in situ* sol-gel hybridization, a process that took another 15 min. Prior to characterization, each sample was dried at 150 °C in a vacuum oven for 3 days to remove residual solvents. The hybrid products were pressed into thin plates using a hot press at 140 °C and were then put into a desiccator for cooling. The cooled plate was then made into standard specimens for characterization.

Characterization of Hybrids

FTIR Analysis

The grafting reaction of acrylic acid onto POE was investigated via Fourier transform infrared spectrometry (BIO-RAD FTS-7PC type) of the thin film specimens. This also allowed verification of the incorporation of a titania and silicate phase to the extent that Ti–O–Si, Ti–O–Ti, and Si–O–Si bonds were formed in the hybrids.

^{29}Si Solid-State NMR Analysis

^{29}Si-NMR spectra were recorded on a Bruker MSL-400 NMR spectrometer, using a standard double air bearing cross polarization/magic angle spinning probe, operated at a frequency of 79.5 MHz for ^{29}Si. Samples were loaded into 4-mm fused zirconia tubes and sealed with Kel-F™ caps. Spectra were obtained at a spinning rate of about 4700 Hz, with other conditions as proposed by Shao et al.[26] The ^{29}Si solid-state NMR spectra were used to study the degree of molecular connectivity of the silicate phase.

XRD Analysis

Analysis of X-ray diffraction intensity curves, recorded with a Rigaku D/max 3V X-ray diffractometer using Co–Kα radiation with a scanning rate of 2°/min, allowed a study of the structural differences between POE, POE-g-AA, and the hybrids.

Dynamic Mechanical Analysis

To study the compatibility of blends, their dynamic mechanical properties were assessed using a TA analyzer Model 2080. The tests were performed at a frequency of 1 Hz, a strain level of 0.075%, and a temperature range of −120 °C to 80 °C with a heating rate of 3 °C/min. To specify the static force (the force exerted in the linear region of elasticity without causing drawing effects), several stress–strain experiments were conducted

beforehand. The ratio of static force to dynamic force was kept constant during the experiments.

DSC Analysis

The glass transition temperature (T_g) of samples was determined using a TA Instrument 2010 DSC system. For DSC tests, sample sizes ranged from 4–6 mg, and the T_g values were obtained from the melting curves taken at a temperature range of −30 °C to 120 °C scanned at a heating rate of 10 °C/min.

TGA Analysis

A thermogravimetry analyzer (TA Instrument 2010 TGA) was used to assess whether organic–inorganic phase interactions influenced thermal degradation of hybrids. Samples were placed in alumina crucibles and tested with a thermal ramp over the temperature range of 30 ~ 600 °C at a heating rate of 20 °C/min and then the initial decomposition temperature (IDT) of hybrids was obtained.

Mechanical Testing

Following the ASTM D638 method, an Instron mechanical tester (Model LLOYD, LR5K type) was used to measure the tensile strength at break. The prepared films, conditioned at 50 ± 5% relative humidity for 24 h prior to the measurements, were prepared in a hydrolytic press at 140 °C, and then measurements were taken using a 20 mm/min crosshead speed. Five measurements were taken for each sample and the results were averaged to obtain a mean value.

RESULTS AND DISCUSSION

Infrared Spectroscopy

Figure 1(A–D) shows the FTIR spectra of POE, POE-g-AA, POE/SiO_2–TiO_2 (10 wt %), and POE-g-AA/SiO_2–TiO_2 (10 wt %). All the peaks characteristic of POE, at 2840–2928, 1465, and 720 cm^{-1}, appear in all four polymers. The modified POE spectrum has two extra peaks (1710 and 1247 cm^{-1}), characteristic of -C═O and -C-O, and a broad O-H stretching absorbance at about 3000 ~ 3600 cm^{-1}. Similar results can be found in other studies.[19,21,27] The appearance of the free-acid based peaks near 1710 and 1247 cm^{-1} in the spectrum of modified POE confirms that acrylic acid had grafted onto POE. More details about the grafting reaction of AA onto POE are given in our previous paper,[21] which also reported how gel formation accompanied the POE-g-AA reaction but that its effect could be neglected because of the low gel yield.

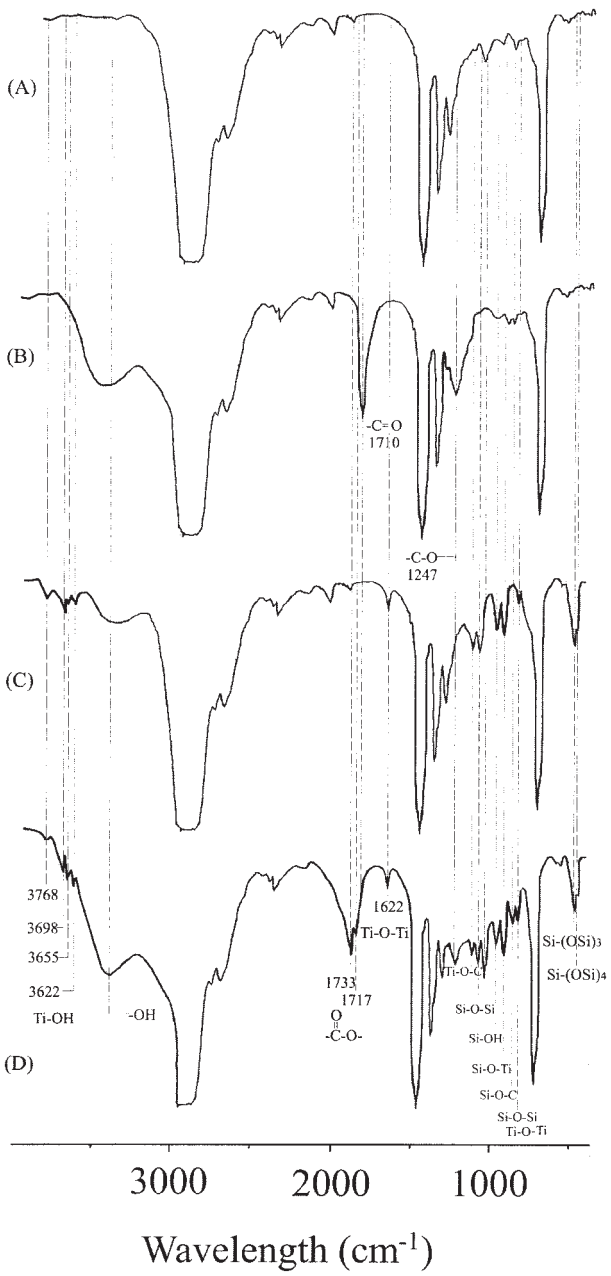

Figure 1. FTIR spectra of (A) pure POE, (B) POE-g-AA, (C) POE/SiO_2–TiO_2 (10 wt %), and (D) POE-g-AA/SiO_2–TiO_2 (10 wt %).

New peaks, at about 3000 ~ 3800, 1000 ~ 1800, 900 ~ 1000, 800 ~ 900, and 400 ~ 500 cm^{-1}, appeared in the FTIR spectrum of the POE/SiO_2–TiO_2 (10 wt %) composite (Figs. 1A–C). The

broad peak at about 3000 ~ 3800 cm^{-1} in the spectra of POE/SiO_2–TiO_2 is due to the existence of O–H groups (Si–OH and Ti–OH) and the formation of hydrogen bonds, while the peaks in the range 1200 ~ 700 cm^{-1} indicate the SiO_2–TiO_2 phase. The peaks between 900 ~ 1800 cm^{-1} are the result of Si–O–Si (1021 and 1080 cm^{-1}), Si–O–Ti (921 cm^{-1}), and Ti–O–Ti (1622 cm^{-1}) bonds. Coordinated bonds between the POE and SiO_2–TiO_2 network (Si–O–C and Ti–O–C) are absent. Based on the above observations, it may be supposed that the interfacial force between the POE matrix and the SiO_2–TiO_2 network is facilitated only by hydrogen bonds. Comparing the spectra of POE-g-AA and POE-g-AA/SiO_2–TiO_2 (Figs. 1B and 1D), it is found that in the former there is a peak at 1710 cm^{-1}. In the latter this is not present, but there are two new peaks, at 1733 and 1717 cm^{-1}. This may be due to the formation of ester groups through the reaction between the carboxylic acid groups of POE-g-AA and the Si-OH/Ti-OH groups of the SiO_2–TiO_2 network.[4,28] Also, there are additional stronger bands at 3622, 3655, and 3698 cm^{-1} in the spectra of POE/SiO_2–TiO_2 (10 wt %) and POE-g-AA/SiO_2–TiO_2, characteristic of tetrahedral coordinated vacancies and designated as $_4Ti^{4+}$-OH, while the band at 3768 cm^{-1} was assigned to octahedral vacancies and designated as $_6Ti^{3+}$-OH. This region at 3600–3800 cm^{-1} was, therefore, identified as representing nonhydrogen bonded Ti–OH groups (labeled as isolated or free hydroxyl groups). The absorbance of free Si–OH groups appeared at a lower region, about 960 cm^{-1}.

To better understand the hydrogen-bonding interaction between the POE-g-AA matrix and the SiO_2–TiO_2 network, FTIR spectra of POE-g-AA copolymer and POE-g-AA/SiO_2–TiO_2 hybrids with different amounts of SiO_2–TiO_2 were expanded in the limited range of 3000 ~ 3600 cm^{-1} (Fig. 2). For the POE-g-AA copolymer (Fig. 2A), the hydroxyl-stretching band appears as a strong broad band at 3445 cm^{-1}. For POE-g-AA/SiO_2–TiO_2 hybrids (Figs. 2B–D), the vibration bands broadened with increased SiO_2–TiO_2 content and shifted to 3418 cm^{-1}, 3401 cm^{-1}, and 3378 cm^{-1} for 3, 10, and 20 wt % SiO_2–TiO_2, respectively. The above observations demonstrate the existence of strong hetero-associated hydrogen bonds between carboxylic acid groups of the POE-g-AA matrix and Si–OH or Ti–OH groups of the SiO_2–TiO_2 network. In addition, because H-bonds between –COOH groups are stronger than those

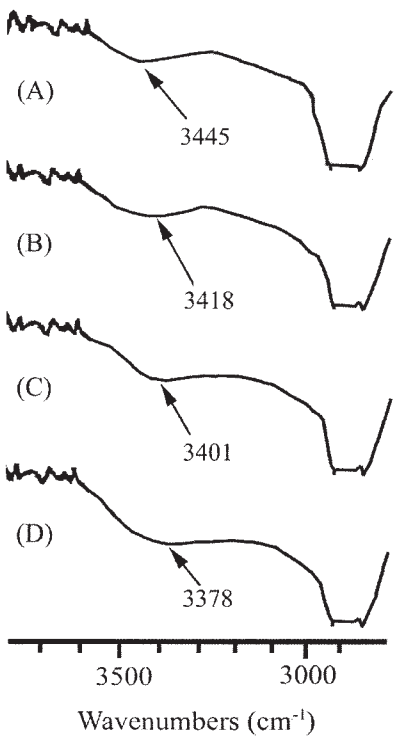

Figure 2. FTIR spectra in the limited range of 3000 ~ 3600 cm^{-1} for (A) POE-g-AA, (B)POE-g-AA/SiO_2–TiO_2 (3 wt %), (C) POE-g-AA/SiO_2–TiO_2 (10 wt %), and (D) POE-g-AA/SiO_2–TiO_2 (20 wt %).

between –COOH and Si–OH or Ti–OH groups, increasing SiO_2–TiO_2 content shifts the wave number to a lower value (lower stretching energy). Another reason for the shift in wave number is the presence of H_2O formed from esterification of –COOH and Si–OH or Ti–OH, which also increases with SiO_2–TiO_2 content. As for the peak broadening, this is attributed to the increasing amount of –OH groups with the increase in SiO_2–TiO_2 content.

The observed stretching vibration of $(Si–O–Si)_{asym}$ (asymmetric) at 1000–1100 cm^{-1} (Fig. 3) represents condensation reactions between Si-OH groups. Noticeably, the $(Si–O–Si)_{asym}$ vibration consists of two components arising from Si–O–Si groups in linear fragments (~ 1021 cm^{-1}) and in loops (~ 1080 cm^{-1}) (indicated "cyclic" in Fig. 3).[26] Consequently, a comparison of linear and cyclic components' absorbance magnitudes contributes to understanding the degree of molecular connectivity within the silicon oxide phase. Meanwhile, the Si-OH vibration absorbance (~ 960 cm^{-1}) is a measure of the number of uncondensed silanol groups. Hence, the relative absorbance of these two types of bands (Si-O-Si and Si-OH) al-

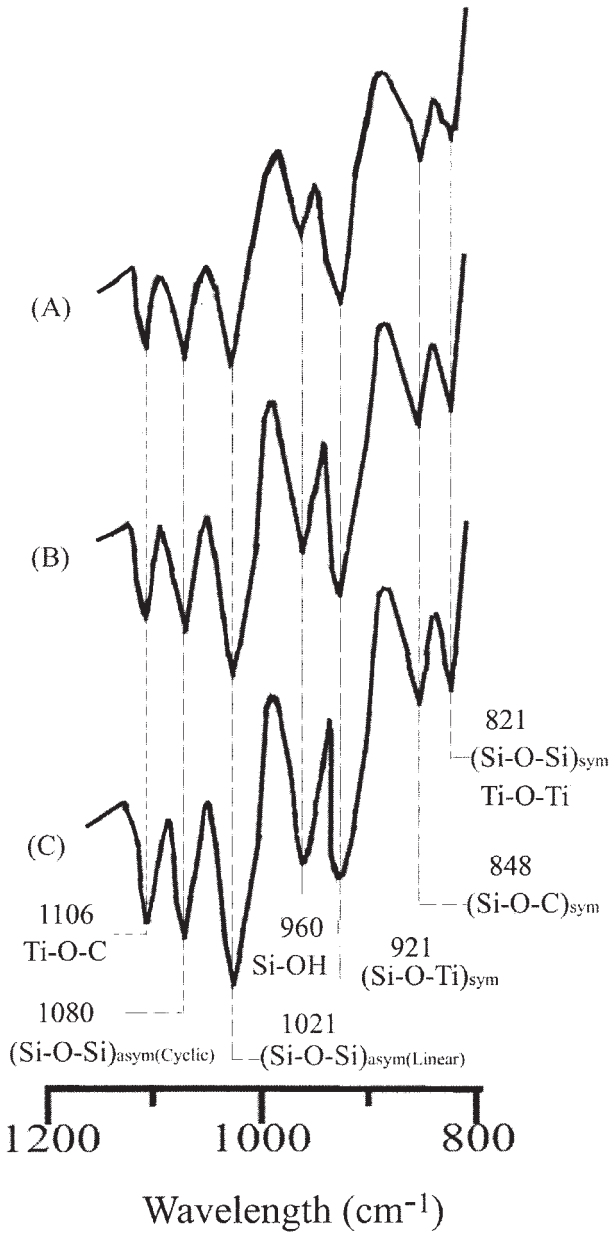

Figure 3. FTIR spectra in the limited range of 800 ~ 1200 cm^{-1} for (A) POE-g-AA/SiO_2–TiO_2 (3 wt %), (B) POE-g-AA/SiO_2–TiO_2 (10 wt %), and (C) POE-g-AA/SiO_2–TiO_2 (20 wt %).

lows an assessment of the degree of crosslinking within incorporated silicon oxide phases. Likewise, comparing absorbance of Ti-O-Ti (1622 and 821 cm^{-1}) and Ti-OH (3600 ~ 3800 cm^{-1}) also allows measurement of the degree of crosslinking of the titania phase.

Another signature of network-forming in the SiO_2–TiO_2 phase is a peak at around 800 cm^{-1}, representing symmetric vibration of Si–O–Si groups ([Si–O–Si] $_{sym}$). Although the symmetric vibration of Si–O–Si is theoretically FTIR inactive, its presence is attributed to distortion of bonding symmetry about the SiO_4 tetrahedral. Furthermore, a strong Ti–O–Ti band is known to exist at 820 cm^{-1} for condensed butoxytitanium; hence, there may be another absorbance peak for the Ti–O–Ti group on the immediate high-frequency side of $(Si–O–Si)_{sym}$. The circumstance of having these two bands in essentially the same position, coupled with lack of high spectral resolution, makes it difficult to ascertain whether the Ti–O–Ti bond actually formed. Nonetheless, the possibility cannot be discounted. The spectra in Figure 3 additionally suggest that absorbance of Si–O–Si groups in loop and linear configuration increased slightly with the SiO_2–TiO_2 content. Increase in absorbance intensity for linear Si–O–Si may be connected with a post reaction with TTIP, leading to the presence of residual alkoxytitanium groups.[12,26] TTIP produces a very strong peak at 1080 cm^{-1} in ethanol, and in this case perhaps also causes the increasing absorbance of the cyclic Si–O–Si group. The absorbance at 848 cm^{-1} is caused by a Si–O–C group, while the peak at 1106 cm^{-1} indicates a Ti–O-C bond, which may be produced from the reaction between POE-g-AA and the titanium bonded isopropyl group.[28]

On further examination of the FTIR spectra, it was found that with increasing SiO_2–TiO_2 content there were two progressively developing peaks at 921 and 960 cm^{-1}. Based on earlier spectroscopic studies of sol-gel-derived glasses by Gonzalez-Oliver et al.,[7] as well as on the studies of Song et al.,[29] the peak at 921 cm^{-1} can be said to represent simple compounds containing the Ti–O–Si group, whereas the peak at 960 cm^{-1} was assigned to the stretching vibration of the Si–OH group. Shao et al.[26] carefully studied the overlapping of this Ti–O–Si band with the Si–OH stretching band and placed them in the same positions as has this study (Fig. 3).

Another interesting trait associated with the POE-g-AA/SiO_2–TiO_2 hybrid appears in the 400 ~ 500 cm^{-1} range of the FTIR spectra. According to the works of Lippert et al.[6] and Wu et al.,[30] the absorbance located in this range is associated with partially condensed intermediates in the polymerization of silicic acid, namely, Si-$(OSi)_2$ (Q_2, 525 cm^{-1}), Si-$(OSi)_3$ (Q_3, 484 cm^{-1}), and Si-$(OSi)_4$ species (Q_4, 432 cm^{-1}). To understand the effect of silica content on this feature, the spectra for POE-g-AA/SiO_2–TiO_2 hybrids with different SiO_2–TiO_2 content were expanded in this limited

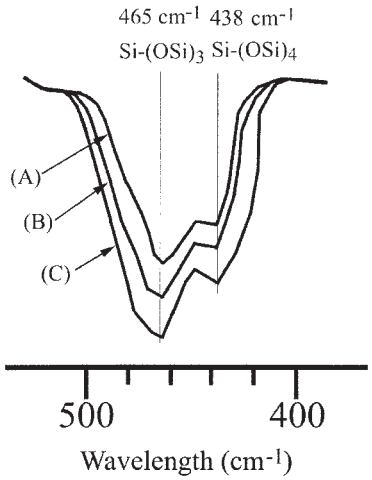

Figure 4. FTIR spectra in the limited range of 400 ~ 500 cm^{-1} for (A)POE-g-AA/SiO_2–TiO_2 (3 wt %), (B) POE-g-AA/SiO_2–TiO_2 (10 wt %), and (C) POE-g-AA/SiO_2–TiO_2 (20 wt %).

range (Fig. 4). The spectra show a peak at about 438 cm^{-1} (Si-$(OSi)_4$), to the right of the peak assigned to the Si-$(OSi)_3$ bending deformation at about 465 cm^{-1}. Moreover, Figure 4 shows that both absorbencies increased with increasing SiO_2–TiO_2 content. This is because the formation of Q_3 and Q_4 increased. Also, the relative intensity of Q_3 and Q_4 varied with SiO_2–TiO_2 content. This was further demonstrated in the results of ^{29}Si solid-state NMR analysis.

^{29}Si Solid-State NMR Spectroscopy

The ^{29}Si solid-state NMR spectra were used to study the degree of molecular connectivity of the silicate phase. Peak assignments for different degrees of Si atom substitution about the SiO_4 tetrahedral have been discussed in earlier studies of organic/silica hybrids.[4,30] Peaks are generally denoted by the symbol Q_n for the Si atom coordination state $(RO)_{4-n}Si(OSi)_n$, where R═H or an alkyl group. Each peak is located within a range of chemical shifts relative to $Si(Me)_4$, as follows: Q_1 = −68 to −83 ppm, Q_2 = −74 to −93 ppm, Q_3 = −91 to −101 ppm, and Q_4 = −106 to −120 ppm. Table 2 and Figure 5 display the results of NMR of POE-g-AA/SiO_2–TiO_2 hybrids containing 3, 10, and 20 wt % SiO_2–TiO_2. It can be seen that the chemical shift distribution consists almost exclusively of Q_3 and Q_4 species, with Q_2 species in evidence at higher SiO_2–TiO_2 content. It could be implied that in hybrids displaying only Q_3 and Q_4 peaks, all the silica has reacted with the POE-g-AA copolymer. On the other hand, the appearance of Q_2 in the spectrum indicates that silica introduced into the hybrid was in excess. Additionally, sufficient Q_2 in the hybrid indicates that the structure has considerable linearity, consistent with the FTIR result (absorbance at 1021 cm^{-1}). Table 2 also shows how Q_2 intensity increased with SiO_2–TiO_2 content at contents above 10 wt %. This is because, at contents above 10 wt %, the silanol groups do not react with POE-g-AA but instead take part in a self-coordination reaction, thus leading to an increase of Q_2. It can also be seen from Figure 5 and Table 2 that the intensity of Q_3 increased, but the intensity of Q_4 slightly decreased with increase of SiO_2–TiO_2 content. This may indicate that Q_4 transformed into Q_3 as the SiO_2–TiO_2 content increased. The relative degree of Q_3 and Q_4 coordination states is in general agreement with the structural interpretation of the FTIR results, and it might be inferred that some degree of porosity is present since "porous" silicate nanoparticles have a considerable degree of intramolecular disconnection.[4,16]

X-ray Diffraction

X-ray diffraction analysis was used to examine the crystalline structures of pure POE, POE-g-AA, and POE-g-AA/SiO_2-TiO_2 (Fig. 6). For unmodified POE (Fig. 6A) there are two peaks, at about 2θ = 19.8° and 2θ = 21.4°. This is similar to the result of Wu et al.[21] The peak at 21.4° represents the orthombic cells of polyethylene, and the peak at 19.8° is considered as indicative of the side branches of octene in the crystalline structure. There is only one peak, at about 2θ = 21.4°, for the POE-g-AA copolymer, compared with two for unmodified POE. The absence of the peak at

Table 2. Relative Proportions of Q_n in POE-g-AA/SiO_2-TiO_2 Hybrids

	Relative Proportions (%)		
SiO_2-TiO_2 (wt %)	Q_2	Q_3	Q_4
3	0	39	61
7	0	43	57
10	0	48	52
13	3	50	47
20	5	51	44

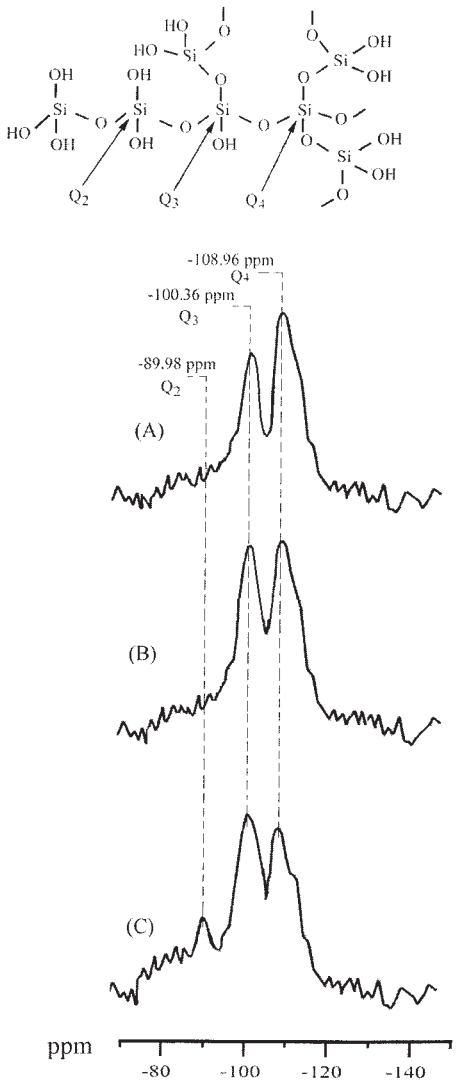

Figure 5. ^{29}Si solid-state NMR spectra of (A) POE-g-AA/SiO_2–TiO_2 (3 wt %), (B) POE-g-AA/SiO_2–TiO_2 (10 wt %), and (C) POE-g-AA/SiO_2–TiO_2 (20 wt %).

about 2θ = 19.8° for the POE-g-AA copolymer may be due to changes in coordination features of POE molecules when acrylic acid is grafted onto POE. Adding to the results of FTIR and XRD, this further confirms that acrylic acid was grafted onto POE.

Compared with POE-g-AA, the XRD spectra of POE-g-AA/SiO_2-TiO_2 hybrids (Figs. 6C–E) show five new peaks, at 2θ = 18.3°, 25.9°, 29.1°, 35.6°, and 41.1°. The appearance of a new peak at 2θ = 18.3°, which may be due to the formation of an ester carbonyl functional group as described in the discussion of FTIR analysis, is similar to the results reported by Wu and Liao[4] and Shogren et al.[31] Moreover, one can refer the appearance of the new peaks at 2θ = 25.9° and 29.1° to the generation of a titanium bonded isopropyl functional group in the anatase and rutile phase.[32,33] The new peak at 2θ = 35.6°, also reported by Kumar et al.,[33] can be assigned to the generation of a titania functional group in the Ti_2O_3 phase. The peak at 41.1°, attributed to the generation of a silanol functional group in the silica network,[4] becomes larger as SiO_2–TiO_2 content increases.

Dynamic Mechanical Analysis

Variations in the tan δ with temperature for the pure POE and for the POE hybrid materials with no chemical bonding to the SiO_2–TiO_2 are shown in Table 3 and Figure 7. The results indicate that with an increase in temperature, onset of segmen-

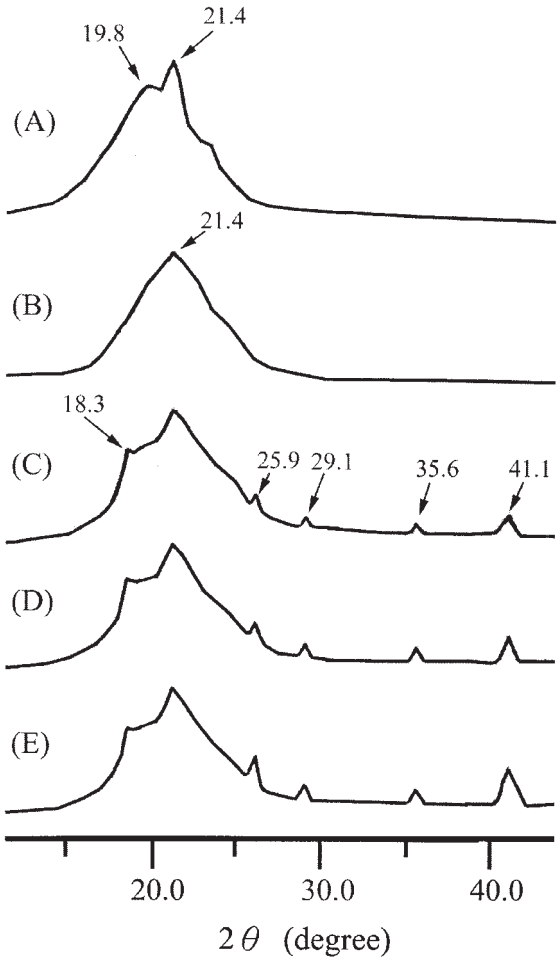

Figure 6. X-ray diffraction spectra for (A) pure POE, (B) POE-g-AA, (C) POE-g-AA/SiO_2–TiO_2 (3 wt %), (D) POE-g-AA/SiO_2–TiO_2 (10 wt %), and (E) POE-g-AA/SiO_2–TiO_2 (20 wt %).

Table 3. Glass Transition Temperature of POE/SiO_2-TiO_2 and POE-g-AA/ SiO_2-TiO_2 Hybrids

TiO_2 (wt %)	POE/SiO_2-TiO_2 $T_{g,\beta}$(°C)	POE-g-AA/SiO_2-TiO_2 $T_{g,\beta}$(°C)
0	−37.2	−34.6
3	−35.3	−30.2
7	−35.0	−26.3
10	−34.2	−21.3
13	−34.5	−27.9
20	−34.8	−32.6

tal motion at a particular temperature leads to a sharp increase in tan δ. The pure POE shows a peak of $T_{g,\beta}$ at around −37.2 °C. In the case of the hybrid material, however, this peak splits into two and shows a displaced maximum. The small peak shifted to a higher temperature, around −35 ± 2 °C, in the hybrid because SiO_2–TiO_2 hinders segmental motions of the polymer chains. Peaks produced by the hybrid broaden and decrease in intensity with increasing SiO_2–TiO_2 content, and the accompanying small shoulders at higher temperatures suggest physical interactions between the inorganic phase and parts of the polymer matrix. Note the inorganic phase can become brittle enough to lower the modulus.

Bonded POE-g-AA/SiO_2-TiO_2 Hybrid Materials

Table 3 and Figure 8 show the variation in tan δ with temperature for pure POE-g-AA and POE-g-AA chemically bonded with the SiO_2–TiO_2 network. With addition of SiO_2–TiO_2, the single sharp peak of the POE-g-AA again splits into a primary peak and a small broad shoulder. However, unlike the hybrid without chemical bonding (Fig. 7), the small shoulder shifts to higher temperatures with increasing SiO_2–TiO_2 content up to 10 wt %, while it decreases noticeably at 20 wt % content. This difference is due to the self-coordination of excess SiO_2–TiO_2 at 20 wt % content, with the subsequent production of a grumous compound causing the shift of temperature to a lower level. More detailed explanation is offered in the following section. A comparison of Figure 8 and Figure 7 shows that the shift of tan δ to higher temperatures is more significant in the POE-g-AA/SiO_2–TiO_2 system. Improved bonding is the reason for this better performance. Our results suggest that there are indeed more chain ends available for bonding of POE-g-AA with SiO_2–TiO_2, and this higher degree of bonding is the origin of the considerable shifts in the $T_{g,\beta}$ values. Conclusively, the maximum interfacial interactions occur at approximately 10 wt % SiO_2–TiO_2 content, as can be identified from Figure 8.

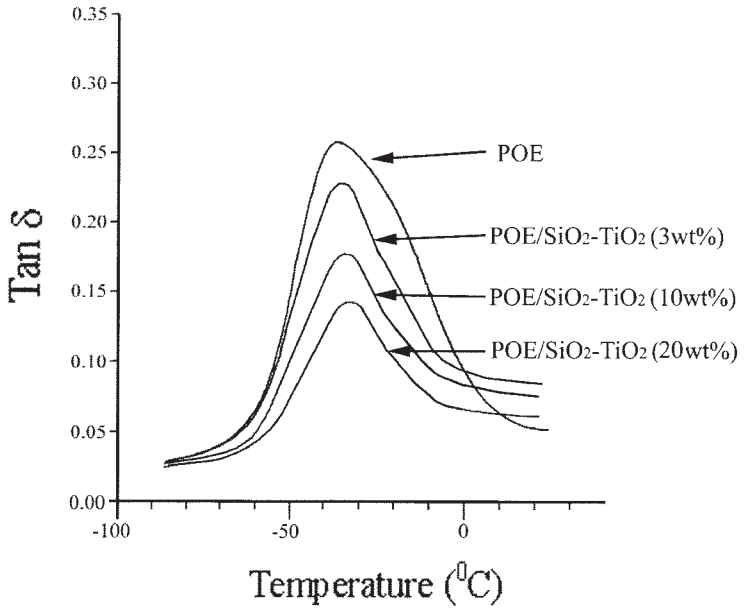

Figure 7. Variation of the loss tangent (tan δ) with temperature for POE/SiO_2–TiO_2 composites.

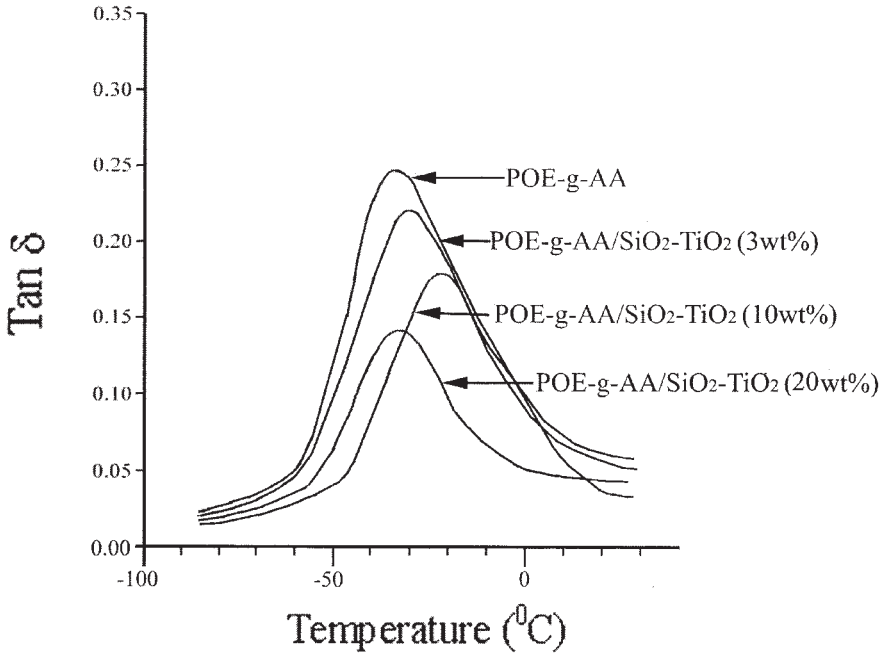

Figure 8. Variation of the loss tangent (tan δ) with temperature for POE-g-AA/SiO_2–TiO_2 composites.

Thermal Stability of Hybrids (DSC and TGA Tests)

It is well known that the thermal stability of organic/inorganic hybrids depends on the interaction between the polymer chains and the inorganic network, and the consequential uniform distribution of the latter in the matrix of the former.[34,35] The thermal properties (T_g and IDT) of hybrids with various SiO_2–TiO_2 content were obtained using DSC and TGA tests, and the results are given in Table 4. The glass transition temperature of the hybrid composites is associated with a cooperative motion of long-chain segments, which may be hindered by the SiO_2–TiO_2 network.[19,36] Hence, as expected, both the POE/SiO_2-TiO_2 and POE-g-AA/SiO_2–TiO_2 hybrids had higher glass transition temperatures than either the POE or the POE-g-AA (Table 4). It was also found that the enhancement in T_g was more significant for POE-g-AA/SiO_2–TiO_2 than for POE/SiO_2–TiO_2. This indicates that the carboxylic acid groups of POE-g-AA provided coordination sites for chemical bonding with the SiO_2–TiO_2 phase. The bonds produced are more able than hydrogen bonds to hinder the motion of the polymer chains.

Additionally, the maximum T_g of POE-g-AA/SiO_2–TiO_2 hybrids occurred at about 10 wt % SiO_2–TiO_2. This may be due to the low grafting percentage (about 5.65 wt %) of the POE-g-AA copolymer, as the increment of T_g depends on the amount of functional groups in the copolymer ma-

Table 4. Thermal and Mechanical Properties of POE/SiO_2-TiO_2 and POE-g-AA/SiO_2-TiO_2 Hybrids

SiO_2-TiO_2 (wt %)	POE/SiO_2-TiO_2			POE-g-AA/SiO_2-TiO_2		
	IDT (°C)	T_g (°C)	TS (MPa)	IDT (°C)	T_g (°C)	TS (MPa)
0	433	−59.8	27.3 ± 0.3	425	−58.6	17.3 ± 0.3
3	438	−58.3	28.2 ± 0.5	456	−53.9	36.6 ± 0.9
7	443	−57.1	29.5 ± 0.6	466	−51.7	41.9 ± 1.0
10	449	−56.2	32.1 ± 0.8	482	−47.8	56.1 ± 1.3
13	453	−57.2	30.5 ± 0.3	487	−52.8	42.6 ± 0.8
20	458	−57.7	27.5 ± 0.2	492	−56.5	29.6 ± 0.5

trix able to react with the residual Si–OH and Ti–OH groups in the SiO_2–TiO_2 network.[37] With SiO_2–TiO_2 content greater than 10 wt %, excess SiO_2–TiO_2 was physically dispersed in the polymer matrix, possibly causing separation between the organic and inorganic phases and reducing compatibility between the inorganic phase and the organic matrix. Hence, the T_g value of POE-g-AA/SiO_2–TiO_2 increased with SiO_2–TiO_2 content to a maximum value and then dropped.

From the results in Table 4, it can be seen that the IDT value of POE-g-AA was lower than that of POE, that both the POE/SiO_2–TiO_2 and POE-g-AA/SiO_2–TiO_2 hybrids had a positive effect on the IDT value, and that the IDT value of POE-g-AA/SiO_2–TiO_2 was higher than that of POE/SiO_2–TiO_2. This result is due to the fact that the interfacial forces between the polymer matrix and the SiO_2–TiO_2 network change from the weaker hydrogen bonds to the stronger carboxylic acid group coordination sites when POE-g-AA is used in place of POE to prepare the hybrids. The increment of IDT with SiO_2–TiO_2 content for POE/SiO_2–TiO_2 and POE-g-AA/SiO_2–TiO_2 hybrids was not significant when the content was greater than 10 wt % (Table 4), because phase separation could occur in the hybrids.

Tensile Strength of Hybrids

Variation in tensile strength at break with SiO_2–TiO_2 content for POE/SiO_2–TiO_2 and POE-g-AA/SiO_2–TiO_2 is also shown in Table 4. Similar to the outcome of thermal stability testing, maximum values for both the POE/SiO_2–TiO_2 and POE-g-AA/SiO_2–TiO_2 hybrids were recorded at about 10 wt % SiO_2–TiO_2. For POE/SiO_2–TiO_2 hybrids, the effect of SiO_2–TiO_2 content on the tensile strength was slight because the interfacial bond between the POE matrix and the SiO_2–TiO_2 network is only the weaker hydrogen bond. The POE-g-AA/SiO_2–TiO_2 hybrid, with the same SiO_2–TiO_2 content, exhibited much better tensile strength than the POE/SiO_2–TiO_2 hybrid, though the POE-g-AA copolymer lowered the tensile strength of pure POE. This clear enhancement in tensile strength may be attributed to the presence of the SiO_2–TiO_2 network and to the formation of chemical bonds, perhaps Si-O-C and Ti-O-C bonds, through the dehydration of carboxylic acid groups in POE-g-AA with the residual Si–OH and Ti–OH groups in the SiO_2–TiO_2 network. Although the tensile strength of the POE-g-AA/SiO_2–TiO_2 hybrid increased to about 56 MPa at 10 wt % SiO_2–TiO_2, it decreased markedly when the concentration of SiO_2–TiO_2 was greater than this. Once again, this is because separation between the organic and inorganic phases occurred in hybrids having high SiO_2–TiO_2 content.

CONCLUSIONS

In this article, organic–inorganic hybrid materials were prepared using an *in situ* sol-gel process. FTIR and XRD spectra showed that the acrylic acid had been grafted onto the POE copolymer and that Si–O–Ti, Si–O–Si, Ti–O–Ti, Ti–O–C, and Si-O-C bonds had formed in the POE-g-AA/SiO_2–TiO_2 hybrid. The newly formed Si-O-C and Ti–O–C bonds may be produced through dehydration of carboxylic acid groups in the POE-g-AA matrix with residual Si–OH and Ti–OH groups in the silica and titania network. It was found, as a result of ^{29}Si solid-state NMR analysis and in agreement with the structural interpretation of FTIR spectra, that Si atom coordination around SiO_4 units is predominantly Q_3 and Q_4. TGA tests showed that the POE-g-AA/SiO_2–TiO_2 hybrids had higher values of initial decomposition temperature than the POE/SiO_2–TiO_2 hybrids. The effect of SiO_2–TiO_2 content on tensile strength and glass transition temperature of POE-g-AA/SiO_2–TiO_2 hybrids was similar. Maximum values of tensile strength and glass transition temperature occurred at about 10 wt % SiO_2–TiO_2; excess SiO_2–TiO_2 particles above this wt % may cause separation between the organic and inorganic phases and so reduce compatibility between the SiO_2–TiO_2 network and POE-g-AA. Finally, the POE-g-AA/SiO_2–TiO_2 hybrids showed improved thermal and mechanical properties over POE/SiO_2–TiO_2 hybrids because the interfacial forces of the former are the stronger Si-O-C, Ti-O-C, and hetero-associated hydrogen bonds, whereas those of the latter are weaker hydrogen bonds.

REFERENCES AND NOTES

1. Hench, L. L.; West, J. K. Chem Rev 1990, 90, 33.
2. Que, W.; Sun, Z.; Zhou, Y.; Lam, Y. C.; Kam, C. H. Thin Solid Films 2000, 359, 177.
3. Aizawa, M.; Nosaka, Y.; Fujii, N. J Non-Cryst Solids 1991, 128, 77.
4. Wu, C. S.; Liao H. T. J Polym Sci: Part B: Polym Phys 2003, 41, 351.

5. Birnie III, D. P.; Bendzko N. J Mater Chem and Phys 1999, 59, 26.
6. Lippert, J. L.; Melpolder, S. M.; Kelts, L. M. J Non-Cryst Solids 1988, 104, 139.
7. Gonzalez-Oliver, C. J. R.; James, P. F.; Rawson H. J Non-Cryst Solids 1982, 48, 129.
8. Mendez-Vivar, J.; Mendoza-Serna, R.; Bosch, P.; Lara, V. H. J Non-Cryst Solids 1999, 248, 147.
9. Karthikeyan, A.; Almeida, R. M. J Non-Cryst Solids 2000, 274, 169.
10. Habsuda, J.; Simon, G. P.; Cheng, Y. B.; Hewitt, D. G.; Diggins, D. R.; Toh, H.; Cser, F. Polymer 2002, 43, 4627.
11. Zhou, W.; Dong, J. H.; Qin, K. Y.; Wei, Y. J Polym Sci: Part A: Polym Chem 1998, 36, 1607.
12. Lu, S.; Melo, M. M.; Zhao, J.; Pearce, E. M.; Kwei, T. K. Macromolecules 1995, 28, 4908.
13. Iwamoto, T., Morita, K.; Mackenzie, J. D. J Non-Cryst Solids 1993, 159, 65.
14. Wang, K. H., Chung, I. J., Jang, M. C., Keum, J. K.; Song H. H. Macromolecules 2002, 35, 5529.
15. Siudak, D. A.; Mauritz, K. A.; J Polym Sci: Part B: Polym Phys 1999, 37, 143.
16. Siudak, D. A.; Start, P. R.; Mauritz, K. A. J Appl Polym Sci 2000, 77, 2832.
17. Perrin, F. X.; Nguyen, V.; Vernet, J. L. Polymer 2002, 43, 6159.
18. Hajji, P.; David, L.; Gerard, J. F.; Pascault, J. P.; Vigier G. J Polym Sci: Part B: Polym Phys 1999, 37, 3172.
19. Wu, C. S.; Liao, H. T. J Appl Polym Sci 2003, 88, 966.
20. Bensason, S.; Nazarenko, S.; Chum, S.; Hiltner, A.; Baer, E. Polymer 1997, 38, 3913.
21. Wu, C. S.; Lai, S. M.; Liao, H. T., M J Appl Polym Sci 2002, 85, 2905.
22. Kaempfer, D.; Thomann, R.; Mulhaupt, R. Polymer 2002, 43, 2909.
23. Abe, Y.; Misono, T.; J Polym Sci: Polym Chem Ed 1983, 21, 41.
24. Abe, Y.; Misono, T. J Polym Sci: Polym Lett Ed 1982, 20, 205.
25. Gunji, T.; Nagao, Y.; Misono, T.; Abe, Y. J Polym Sci: Polym Chem Ed 1992, 30, 1779.
26. Shao, P. L.; Mauritz, K. A.; Moore, R. B. J Polym Sci: Part B: Polymer Phys 1996, 34, 873.
27. Wu, C. S.; Liao, H. T. M. J Appl Polym Sci 2002, 86, 1792.
28. Wu, C. S. J Appl Polym Sci 2004, 92, 1749.
29. Song, Y. C.; Hasegawa, Y.; Yang, S. J.; Sato, M. J Mater Sci 1998, 23 1911.
30. Wu, K. H.; Chang, T. C., Yang, J. C.; Chen, H. B. J Appl Polym Sci 2001, 79, 965.
31. Shogren, R. L.; Thompson, A. R.; Felker, F. C.; Harry-Okuru, R. E.; Gordon, S. H.; Green, R. V.; Gould, T. M. J Appl Polym Sci 1992, 44 1971.
32. Pottier, A.; Chaneac, C.; Tronc, E.; Mazerolles, L.; Jolivet, J.-P. J Mater Sci Chem 2001, 11, 1116.
33. Kumar, P. M.; Badrinarayanan, S.; Sastry, M. Thin Solid Films 2000, 358, 122.
34. Wei, Y.; Yang, D.; Bakthvatchalam, R. Mater Lett 1992, 13, 261.
35. Hsiue, G.-H.; Chen, J.-K.; Lin, Y.-L J Appl Polym Sci 2000, 76, 1609.
36. Hsu, Y. G.; Chiang, I. J.; Perrier, C.; Lo, J. F. J Appl Polym Sci 2000, 78, 1179.
37. Huang, Z. H.; Qju, K. Y. Polymer 1997, 38, 521.